

# DYNAMICS OF THREE-BLOCK ASSEMBLIES WITH UNILATERAL DEFORMABLE CONTACTS. PART 1: CONTACT MODELLING

UGO ANDREAUS\* AND PAOLO CASINI

*Dipartimento di Ingegneria Strutturale e Geotecnica, Facoltà di Ingegneria, Università degli Studi di Roma 'La Sapienza',  
Via Eudossiana 18, 00184 Rome, Italy*

## SUMMARY

As far as the dynamics of multibody systems is concerned, a brief review has been performed in order to frame the dynamic response of a trilith (the simplest scheme of a colonnade belonging to a temple) into a wide theoretical background. Under the assumption of rigid bodies, two different approaches can be found in the literature: rigid or deformable contacts formulation. In this paper, an effort is made at outlining the principle of rigid contact formulation and of deformable contact formulation. The latter approach can be assumed within the framework of the distinct element method; for this purpose a model of deformable contact has been proposed in order to simulate the real behaviour of stone joints. The sample application referred to the trilith will be presented in Part 2. Copyright © 1999 John Wiley & Sons, Ltd.

KEY WORDS: multibody systems; unilateral constraints; impact; friction; dynamics; distinct element method

## 1. INTRODUCTION

The dynamic analysis of structures composed of rigid blocks has been studied for a number of technical and theoretical reasons. From a technical point of view, for instance, the interest on this topic is connected to the necessity to evaluate the seismic stability of several structures (ranging from tombstones to water tanks, to nuclear plants or to monumental buildings) and to study the behaviour of man-made objects, piece of machinery or any block-like structure with unilateral constraints resting on a moving support. From a theoretical point of view the problem is highly interesting for several aspects related to complex dynamics (periodic trajectories, bifurcations, chaotic behaviour, etc.) and to the existence, uniqueness and continuous dependence on initial conditions of solutions.<sup>1</sup>

A discontinuous medium is distinguished from a continuous one by the existence of contacts or interfaces between the discrete bodies that comprise the system. Discontinuum methods can be

---

\* Correspondence to: Ugo Andreaus, Dipartimento di Ingegneria Strutturale e Geotecnica, Facoltà di Ingegneria, Università degli Studi di Roma 'La Sapienza', Via Eudossiana 18, Rome I-00184, Italy.

Contract grant/sponsor: Italian Ministry of University and Scientific Research.

categorized both by the way they represent contacts and by the way they represent the discrete bodies in the formulation. A model must represent two types of mechanical behaviour in a discontinuous system: (i) behaviour of the discontinuities and (ii) behaviour of the solid material. First, the model must recognize the existence of contacts or interfaces between the discrete bodies that comprise the system. Methods are divided into two groups by the way in which they treat behaviour in the normal direction of motion at contacts. In the first group (using a rigid contact approach) interpenetration is regarded as non-physical. In the second group (using a deformable contact approach), a finite normal stiffness is taken to represent the measurable stiffness that exist at a contact. In both cases the contact locations must be identified in the model. The second type of mechanical behaviour that the model must represent is the behaviour of the solid material that constitutes the bodies in the discontinuous system. There are two main divisions in this representation: the material may be assumed rigid or deformable. The assumption of material rigidity is a good one when most of the deformation in a physical system is accounted for by movement on discontinuities. The movements consist mainly of sliding rotation of bodies and of opening and interlocking of interfaces. If the deformation of the solid material cannot be neglected, deformability can be included by dividing the body into internal elements or boundary elements in order to increase the number of degrees-of-freedom.

A class of methods collectively described as discrete element methods<sup>2</sup> provides the capability to represent the motion of multiple, intersecting discontinuities allowing finite displacements and rotations of discrete bodies (including complete detachment), and recognizing new contacts automatically as the calculation progresses. Two main classes of methods can be identified that conform to the definition of a discrete element method:<sup>2</sup>

Impulse-exchange methods assume both the contacts and bodies to be rigid; impulse is exchanged between two contacting bodies during an instantaneous collision. This formulation is based of the fundamental works of Levi-Civita,<sup>3</sup> Signorini,<sup>4</sup> P  r  s,<sup>5</sup> L  tstedt,<sup>6,7</sup> Moreau,<sup>8</sup> Jean and Moreau,<sup>9</sup> Panagiotopoulos,<sup>10</sup> Pfeiffer and Glocker,<sup>11</sup> Sinopoli.<sup>12</sup>

Distinct element methods, as proposed by Cundall and Hart,<sup>2</sup> use an explicit time-marching numerical scheme to solve the equations of motion directly; bodies may be rigid or deformable (by subdivision into elements); contacts are deformable.

Contact rigidity allows simplification of the dynamical contact–impact problem, but at the same time involves some deep mathematical problems related to existence, uniqueness, and approximating procedures of solutions of problems with unilateral constraints, or *non-smooth* dynamics. The formulation of multibody dynamics with rigid contacts can be the theoretical basis to develop new sophisticated models of contact–impact laws based on finite, boundary, and distinct element methods.<sup>1</sup>

The aim of the present paper is to propose a model of deformable contact which is suitable to analyse contact–impact problems between interacting rigid bodies. Deformability is limited at joint surfaces and is taken into account by means of contact forces concentrated at a discrete number of physical contacts. Refined analytical force-relative displacement relations in either normal and tangential directions with respect to the contact surfaces are formulated which allow to account for (i) detachment and hysteresis in normal direction, (ii) coupling between shear strength and compressive force, friction and damage in tangential direction.

This model (Section 4) will have the framework of the distinct element method (Section 3) and a sample application referred to the dynamic analysis of a trilith will be worked out in Part 2. Furthermore, in Section 2 a synthetic review concerning the formulation of multibody dynamics

with rigid contacts will be presented, which can be used as the theoretical foundation for all the solution algorithms, including those dealing with deformable contact models.

## 2. RIGID CONTACT FORMULATION

### 2.1. Generalities

For dynamical systems of mechanics involving rigid unilateral contacts, the following complementarity situation exists:<sup>11</sup> non-zero relative kinematics (distance, velocity, acceleration) with respect to a contact is accompanied by zero mechanical interactions (forces, momenta) and indicates a passive constraint situation. Zero relative kinematics with respect to a contact is accompanied by non-zero mechanical interactions and indicates an active constraint situation. Thus, the product of magnitudes representing relative kinematics and of magnitudes representing mechanical interaction is always zero. Different but equivalent formulations have been proposed which anyway result in two subproblems, the normal and the tangential, related to unilaterality and friction, respectively.<sup>1,12</sup>

In this section, we will describe the basic complementarity formulations for contacts and collisions with or without friction. The complementarity can be defined between the contact force and the velocity<sup>6-10,12</sup> or the acceleration.<sup>11</sup> Other possible complementarity formulations can be found in Reference 1 and references therein.

The dynamics of a multibody system is usually described by using a set of generalized co-ordinates  $\mathbf{q}$ . This means here that the system is uniquely determined by such a  $\mathbf{q}$  if all contacts show separation. Unfortunately the structure of the dynamical equations is not constant because the contact configuration of the system changes with time due to stick-slip transitions, impacts, and contact losses.<sup>5,8,11</sup>

### 2.2. Contact mechanics

If the contour of each body is assumed to be smooth enough, for each couple of bodies about to collide, it is possible to define the normal  $\mathbf{n}$  and the tangent  $\mathbf{t}$  in each couple of points bounded to collide and to orient the two orthonormal bases antiparallel to each other<sup>11</sup> (Figure 1(c)). The distance  $u_n$  of the contact points in the normal direction is positive for separation and negative for overlapping (Figures 1(a) and 1(b)). For two contact points,  $\dot{u}_n$ ,  $\dot{u}_t$  and  $\ddot{u}_n$ ,  $\ddot{u}_t$  denote the relative velocities and accelerations in normal and tangential directions, respectively (the superimposed dot means differentiation with respect to time). It should be noted that every relative velocity, acceleration or variation can be expressed in a linear manner by the corresponding terms of the generalized co-ordinates.<sup>5,8,11,12</sup>

The terms  $\lambda_n$  and  $\lambda_t$  represent the scalar magnitudes of the normal and tangential contact forces.

### 2.3. Smooth dynamics

**2.3.1. Kinematics.** It may be noted here that a negative value of  $\dot{u}_n$  corresponds to an approaching process of the bodies and coincides at vanishing distance  $u_n = 0$  with the relative velocity in

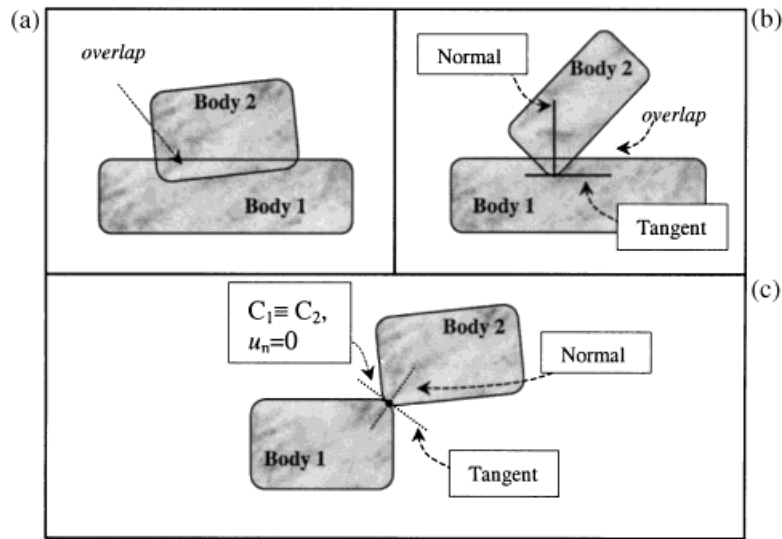


Figure 1. Interface models. (a) Edge-to-edge; (b) corner-to-edge; (c) corner-to-corner

the normal direction before an impact. In the case of a continual contact ( $u_n = \dot{u}_n = 0$ ), the term  $\dot{u}_t$  shows the relative sliding velocity of the bodies, which can be used to determine the time points of transition from sliding ( $\dot{u}_t \neq 0$ ) to sticking or rolling ( $\dot{u}_t = 0$ ).

Contact between two bodies is only maintained if the distance  $u_n$  and the normal relative velocity  $\dot{u}_n$  are equal to zero for all times  $t$ . In particular  $\dot{u}_n = 0$  must not change, which can be accounted for by the additional conditions  $\ddot{u}_n = 0$ . On the other hand, a transition from continual contact ( $u_n = \dot{u}_n = 0$ ) to separation demands velocities greater than zero,  $\dot{u}_n > 0$ , which are only achieved by  $\ddot{u}_n > 0$ . Similarly, this behaviour can be transferred to the tangential constraint. A sticking or rolling contact fulfils  $u_n = \dot{u}_n = \dot{u}_t = 0$  and will continue to stick only if, in addition,  $\ddot{u}_n = \ddot{u}_t = 0$  holds. Transitions to sliding ( $\dot{u}_t \neq 0$ ) are only possible if the tangential relative acceleration  $\ddot{u}_t$  becomes unequal to zero.

**2.3.2. Contact law for normal constraints.** Each closed contact constraint is characterized by a vanishing distance  $u_n = 0$  and normal relative velocity  $\dot{u}_n = 0$ . Under the assumption of impenetrability ( $u_n \geq 0$ ), only two situations may occur: contact is maintained (a) or a transition to separation takes place (b).

- (a) In the first case we know that the relative acceleration must be equal to zero and the normal contact forces must act with a compressive magnitude due to the unilateralness of the normal constraint

$$\ddot{u}_n = 0 \quad \text{and} \quad \lambda_n \geq 0 \quad (1)$$

The condition  $\ddot{u}_n = 0$  ensures that the contact is maintained. Since  $\dot{u}_n = \ddot{u}_n = 0$  the values  $u_n = 0$  never change. The admissible values of the contact forces are given by  $\lambda_n \geq 0$ . A contact force  $\lambda_n < 0$  would correspond to a pulling force and must be excluded.

- (b) The second case describes the separation of the bodies. Separation is only achieved by positive values of the normal relative acceleration and vanishing normal forces

$$\ddot{u}_n \geq 0 \quad \text{and} \quad \lambda_n = 0. \quad (2)$$

We remember that the state of separation is indicated by distances greater than zero,  $u_n > 0$ . Starting from  $u_n = \dot{u}_n = 0$  such a transition occurs only for  $\ddot{u}_n > 0$ . Necessarily compressive contact forces must not be transmitted at separation, because otherwise we would have continual contact. This leads to the second condition  $\lambda_n = 0$ .

From equations (1) and (2) we see that the normal contact law states a complementary condition in acceleration.<sup>11</sup>

$$\lambda_n \geq 0, \quad \ddot{u}_n \geq 0, \quad \lambda_n \ddot{u}_n = 0 \quad (3)$$

The complementarity formulation in acceleration can equivalently be rewritten in velocity form.<sup>1,6-10,12</sup> Maintenance of contact in the motion that follows depends on the value of the velocity  $\dot{u}_n$ . If it is zero, the reactive force  $\lambda_n$  must act to satisfy the relation

$$\dot{u}_n = 0 \quad \text{and} \quad \lambda_n \geq 0 \quad (4)$$

On the contrary, contact will be lost if  $\dot{u}_n > 0$  with

$$\dot{u}_n > 0 \quad \text{and} \quad \lambda_n = 0 \quad (5)$$

Consequently, the normal contact law stating a complementarity condition in velocity is:

$$\lambda_n \geq 0, \quad \dot{u}_n \geq 0, \quad \lambda_n \dot{u}_n = 0. \quad (6)$$

**2.3.3. Contact law for tangential constraints.** The tangential contact state of the possible sticking constraints will be done with respect to the frictional law of Coulomb, which, however does not mean a restriction of generality. With regard to friction the following three cases are possible:

$$\begin{aligned} \dot{u}_t = 0 &\Rightarrow |\lambda_t| \leq \mu_0 \lambda_n \quad (\text{sticking}) \\ \dot{u}_t < 0 &\Rightarrow \lambda_t = \mu \lambda_n \quad (\text{negative sliding}) \\ \dot{u}_t > 0 &\Rightarrow \lambda_t = -\mu \lambda_n \quad (\text{positive sliding}) \end{aligned} \quad (7)$$

This law states that during sliding the friction force is proportional to the normal force of a contact. For sliding friction, we have

$$\lambda_t = -\mu \lambda_n \operatorname{sign}(\dot{u}_t) \quad (8)$$

where the coefficient of friction may depend additionally on the tangential relative velocity,  $\mu = \mu(\dot{u}_t)$ . During sliding the tangential friction force is directed oppositely to the relative velocity  $\dot{u}_t$ . For static friction ( $\dot{u}_t = 0$ ) the values of the tangential force are bounded by the normal force,  $|\lambda_t| \leq \mu_0 \lambda_n$ . Most material pairings in technical practise possess a friction such that we may realistically assume that in transition point from sticking to sliding and *vice versa*, the friction coefficients are the same  $\mu_0 = \mu(\dot{u}_t = 0)$ . We shall therefore use  $\mu_0$  for all transition events. A representation of equation (7) on acceleration level can be given<sup>11</sup> in order to obtain (together with the dynamics equation and the unilateral impenetrability condition in normal direction) a Linear Complementarity Problem (LCP) formulation of the fully coupled state transition problem.

As far as the representation on velocity level is concerned, the general contact law, involving both normal and tangent reactions, becomes<sup>12</sup>

$$\lambda_t = \lambda_n = 0 \quad \text{when} \quad \dot{u}_n > 0 \quad (9)$$

whereas,

$$\lambda_n \dot{u}_n = 0, \quad \lambda_t \dot{u}_t \leq 0 \quad \text{when} \quad \dot{u}_n = 0 \quad (10)$$

In Section 2.5 mention of the influence of the Coulomb friction on the conditions of existence and uniqueness will be made.

## 2.4. Non-smooth dynamics

**2.4.1. Basic assumptions.** Bodies which are initially separated may come into contact. This process is called an impact and involves unsteady changes in the velocities. Normally, two bodies approach each other with a non-zero relative velocity in the normal direction until the distance between them has been vanished. There are several possibilities: the bodies may separate immediately after the collision with a finite positive normal relative velocity, or they may remain in contact. The first case is usually referred to a partly inelastic shock which might be fully elastic if the absolute values of the normal relative velocities before and after the impact are the same. In the second case, the normal relative velocity, which is negative before the impact, jumps to zero and thus enables the bodies to stay together. This type of an impact is called completely inelastic. In both cases, the velocity jumps are enforced by infinite values of the contact forces during the infinitely small time interval of the impact. These impulsive forces are, of course, not restricted to act only in the normal directions. Even in the tangential directions such impulses are transferred and cause velocity jumps there.

Some general assumptions are made:

- (i) the duration of the impact is 'very short'.
- (ii) The bodies undergo a deformation at the impact points, but this deformation is local only (i.e. it is negligible at the bodies' scale). It results from the fact that, due to the infinitely strong impact forces, each of the contact zone becomes elastic. Therefore, during the impact the assumption of rigid constraints must be locally dropped.
- (iii) During the impact the accelerations in the normal directions  $\ddot{u}_n$  are not restricted to any sign.
- (iv) A restriction of the admissible values of the normal impulse to  $\Lambda_n \geq 0$  seems to be reasonable.
- (v) The impact can be divided into two phases: the compression phase (index C) and expansion phase (index E).
- (vi) The compression phase starts at time  $t_0$  and ends at time  $t_C$ . The end of the compression equals the start of the expansion phase. Expansion is finished at time  $t_E$ , which is also the end of the impact.
- (vii) If the distance  $u_n$  in the normal direction becomes zero at one time instant  $t_0$  and the corresponding relative velocity  $\dot{u}_n$  is less than zero, an impact occurs. The impact contact is then closed and the unilateral constraint is active. At the end of the compression the approaching process of the bodies is completed and the end of compression is given by  $\dot{u}_n(t_C) = 0$ .

- (viii) The impulse  $\Lambda_n$  corresponds to the normal impulse that terminates the compression phase.
- (ix) After the process of the expansion, the relative velocity must show positive value  $\dot{u}_n(t_E) \geq 0$ , because negative relative velocities at the end of the impact would lead to a further approach of the bodies and thus to penetration.
- (x) While the impact takes place all magnitudes of the multibody system for position and orientation as well as non-impulsive forces and torques remain constant.

We take into account all active unilateral constraints, which means all the sliding and sticking continuous contact constraints ( $u_n = \dot{u}_n = 0$ ) as well as the impact contact ( $u_n = 0, \dot{u}_n < 0$ ). This enables us to examine whether a contact separates under the influence of an impact at a different location in the multibody system.

#### 2.4.2. Phase of compression.

*Normal behaviour.* The normal impulse of compression results from an integration of the normal force over the phase of compression

$$\Lambda_{nC} = \lim_{t_C \rightarrow t_0} \int_{t_0}^{t_C} \lambda_n dt \quad (11)$$

where due to the unilateral character of the contact constraints only compressive forces are possible.

$$\lambda_n(t) \geq 0, \quad \forall t \in [t_0, t_C] \quad (12)$$

Thus, integrating (equation (11)) the normal forces with property (12) results unambiguously in non-negative values of the normal impulses.

$$\Lambda_{nC} \geq 0 \quad (13)$$

At the end of compression, negative values of the relative velocity are forbidden:

$$\dot{u}_{nC} \geq 0 \quad (14)$$

If an impulse is transferred ( $\Lambda_{nC} > 0$ ), then the corresponding contact participates in the impact and the end of compression is given by  $\dot{u}_n(t_C) = 0$ . If no impulse is transferred ( $\Lambda_{nC} = 0$ ), then the corresponding constraints are superfluous. Thus we allow velocities  $\dot{u}_{nC} \geq 0$ . This behaviour can be completely expressed by the single complementarity condition:

$$\Lambda_{nC} \dot{u}_{nC} = 0 \quad (15)$$

*Tangential behaviour.* The tangential impulse can be derived by integration

$$\Lambda_{tC} = \lim_{t_C \rightarrow t_0} \int_{t_0}^{t_C} \lambda_t dt \quad (16)$$

Integrating Coulomb's law, equation (7) within  $[t_0, t_C]$  states the impact law in the tangential direction:

$$\begin{aligned} \dot{u}_t = 0 &\Rightarrow |\Lambda_{tC}| \leq \mu_0 \Lambda_{nC} \quad (\text{sticking}) \\ \dot{u}_t < 0 &\Rightarrow \Lambda_{tC} = \mu \Lambda_{nC} \quad (\text{negative sliding}) \\ \dot{u}_t > 0 &\Rightarrow \Lambda_{tC} = -\mu \Lambda_{nC} \quad (\text{positive sliding}) \end{aligned} \quad (17)$$

Unfortunately, though equation (17) is fulfilled, there might be time instants within  $[t_0, t_c]$  where the tangential forces  $|\lambda_t|$  exceed the values of  $\mu\lambda_n$ . Moreover, possible stick–slip transitions during the collision with reversed sliding prevent an analytical general integration of equation (7) over the impact interval, so no representation of the friction impulses can be given to determine the relative velocities at the end of compression according to Coulomb's law.

The tangential impact law, equation (17), coincides with Coulomb friction, equation (7), only in the cases of continuous sliding during compression and transition to sticking at the end of compression.

#### 2.4.3. Phase of expansion.

*Normal behaviour.* For the impact constraint in the normal direction, the Poisson's hypothesis states that the impulse  $\Lambda_{nC}$  acting during compression is reduced by the coefficient of restitution  $0 \leq \varepsilon_n \leq 1$  and is then applied to the contact as an expansion impulse  $\Lambda_{nE}$ :

$$\Lambda_{nE} = \varepsilon_n \Lambda_{nC} \quad (18)$$

After the process of expansion, the relative velocity must show positive values

$$\dot{u}_{nE} \geq 0 \quad (19)$$

because negative relative velocity at the end of the impact would lead to a further approach of the bodies and thus to penetration.

The complete impact law during expansion can be stated by the complementarity

$$\Lambda_{nP} \geq 0, \quad \dot{u}_{nE} \geq 0, \quad \Lambda_{nP} \dot{u}_{nE} = 0 \quad (20)$$

where  $\Lambda_{nP}$  is the expansion impulse increment with respect to the Poisson impulse, equation (18), which could be needed to prevent penetration.

*Tangential behaviour.* The tangential behaviour during expansion may be formulated in the same way as during compression only if impulses related to dry friction act on the bodies. The resulting impact law could be the same as in equation (17) by simply replacing the indices C (Compression) by E (Expansion). An advanced modelling enables us to also take into account reversible portions of the tangential impulse which may occur when, after compression, a certain amount of the transferred impulse may be stored in the bodies as elastic deformation, and may lead to a change in the sliding direction during expansion.<sup>11</sup>

#### 2.5. Linear complementarity problem

The complementarities and sign limitations stated in Sections 2.3 and 2.4 together with the equations of motion<sup>5,8,11</sup> for continuous contacts and the equations of impulses<sup>8,11</sup> during the impacts phases can be suitably assembled in order to formulate a LCP, whose structure can be put in the standard form

$$\mathbf{y} = \mathbf{Ax} + \mathbf{b}, \quad \mathbf{y} \geq 0, \quad \mathbf{x} \geq 0, \quad \mathbf{x} \cdot \mathbf{y} = 0 \quad (21)$$

It is worth noting that, for frictionless dynamics, equations (21) can be identified as the Kuhn–Tucker conditions satisfied by the optimal solution of a quadratic programming problem.<sup>1,6,7,11,12</sup> Moreover, the Quadratic Program related to the LCP is an expansion of the principle of least constraints to the unilateral case where both continual contact and the take-off transition are included.<sup>11,12</sup>



In the presence of friction,<sup>1,12</sup> sufficient conditions for existence and uniqueness of the solution were given by Lötstedt,<sup>6,7</sup> who demonstrated that the fulfilment of the Coulomb law is equivalent to the Kuhn–Tucker conditions of a quadratic problem; hence, under appropriate assumptions concerning the position of the system, the problem corresponds to the minimization of a convex function over a convex set, implying the existence of a unique solution.

The formulation involving accelerations possesses the advantage of the possibility of including directly the dynamical equations in the complementarity problem. However, the contact law stating a complementarity condition in velocity, allows the accelerations to be determined without any direct evaluation of the contact forces.<sup>12</sup> In this respect, a variational formulation for the contact dynamics with friction and a geometric method of solution have been proposed by Sinopoli<sup>12</sup> and applied, for instance, to study the starting mechanism of a rigid block at rest on a moving boundary.

### 3. DEFORMABLE CONTACT FORMULATION

#### 3.1. Generalities

In this approach<sup>2</sup> joints between discrete bodies are viewed as interfaces which exchange contact forces due to relative displacements and velocities between contact points. The method alternates between application of a force–displacement law at all contacts and Newton–Euler laws at all bodies. The force–displacement law is used to find contact forces from known displacements. Newton–Euler laws give the motion of the bodies resulting from the known forces acting on them.

#### 3.2. Equations of motion

The motion of an individual body is determined by the magnitude and direction of resultant out-of-balance moments and forces acting on it. It is best to write the equations of motion in an arbitrary non-inertial frame that is both translating and rotating; let us choose the origin of the frame as the centre of mass  $G$  of the body and the axes so that the inertia tensor  $\mathbf{I}_G$  is diagonal. Thus the equations of linear and angular momentum read as follows:

$$\begin{aligned}\mathbf{M}\dot{\mathbf{v}}_G - \sum_i \mathbf{f}_i &= \mathbf{0} \\ \mathbf{I}_G \dot{\boldsymbol{\omega}} - \sum_i \mathbf{P}_i \mathbf{f}_i &= \mathbf{0}\end{aligned}\tag{22}$$

$\mathbf{v}_G$  is the velocity vector of the body centroid,  $\boldsymbol{\omega}$  is the angular velocity of the body,  $\mathbf{M}$  is the diagonal mass tensor,  $\mathbf{f}_i$  are the external forces applied to the body which comprise both active and contact forces,  $\mathbf{P}_i$  is the skew tensor associated with the location vector of the 'ith' force.

#### 3.3. Contact mechanics

**3.3.1. Contact geometry.** A joint is represented as a contact surface (composed of individual point contacts) formed between two body edges. In general, for each pair of bodies that touch

(or is separated by a small enough gap), adjacent bodies can touch along a common edge segment (Figure 1(a)) or at discrete points where a corner meets an edge (Figure 1(b)) or another corner (Figure 1(c)). Physically edge-to-edge contact is important because it corresponds to the case of a joint closed along its entire length. A physical edge-to-edge contact corresponds to a domain with two discrete contacts. The joint is assumed to extend between the two contacts and divided into two halves with each half-length supporting its own contact force.

The usual assumption that body corners are sharp or have infinite strength is unrealistic because of the crash of the corners as a result of a stress concentration. A realistic representation can be achieved by rounding the corners so that bodies can smoothly slide past one another when opposite corners interact. The directions of normal and tangential vectors at each corner-to-edge (Figure 1(b)) or corner-to-corner (Figure 1(c)) contact are defined with respect to the direction of the contact normal.

*3.3.2. Contact kinematics and dynamics.* Assumption (ii) in Section 2.4 of local deformability during impact can be extended to the whole contact phases and the overlap shown in Figure 1(b) is allowed; it represents a mathematically convenient way of measuring relative normal displacement. This is the deformable contact assumption quoted in Section 1. Obviously, unlike the assumption of rigid contact model (Section 2), a negative relative distance between adjacent bodies at contact points gains physical meaning. The directions of normal and shear forces acting at each corner-to-edge or corner-to-corner contact are defined with respect to the direction of the contact normal, as illustrated in Figure 1(b) and 1(c). The deformable contact formulation allows to use contact laws in normal and tangential directions more suitable for the problem and the material pairings under examination. In the following section, refined contact laws will be formulated and roughness parameters will be identified with reference to stone-block assemblies.

## 4. PROPOSED MODEL

In the present paper, a model of deformable contact is proposed which is suitable for use in the study of multibody dynamics with unilateral constraints;<sup>13</sup> a sample application will be presented in the Part 2 with reference to a trilith.

### 4.1. Contact law in normal direction

The normal loading tests have demonstrated that the force–displacement relations for a wide range of natural<sup>14,15</sup> and artificial<sup>16</sup> joint types are invariably non-linear throughout repeated loadings. A hyperbolic function which has been used to fit the stress–strain (lower and upper) envelope curves of soils<sup>17,18</sup> and rocks,<sup>19</sup> as well as truck suspension systems,<sup>16</sup> has the following basic form, Figure 2(a) (solid lines):

$$\Lambda_n(u_n) = k_{ni} U_n \frac{u_n}{u_n - U_n} \quad (23)$$

where  $u_n$  ( $u_n \leq 0$ ) is the contact closure,  $\Lambda_n$  is the compressive force,  $k_{ni}$  the initial stiffness and  $U_n$  ( $U_n < 0$ ) the limit overlap. The values of  $k_{ni}$  and  $U_n$  uniquely define the hyperbolic normal

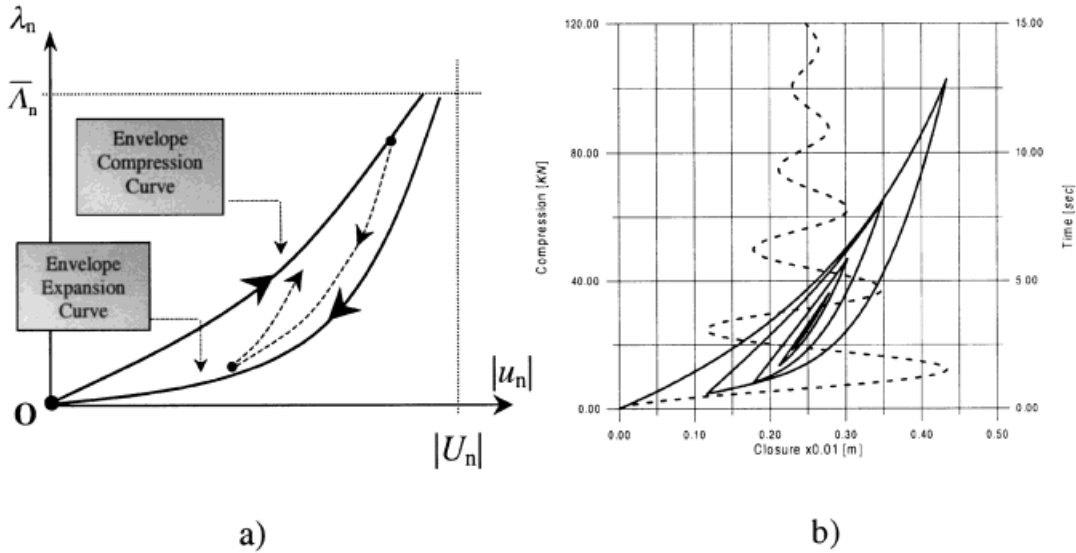


Figure 2. Contact law in normal direction. (a) Envelope curves; (b) cyclic behaviour

force *vs* closure curve characterizing the behaviour of the deformable joints. The tangent stiffness is given by

$$k_n = \frac{\partial \Lambda_n}{\partial u_n} = \frac{k_{ni}}{(1 - (\Lambda_n / (k_{ni} U_n + \Lambda_n)))^2} \quad (24)$$

representing the observed increase of stiffness with compressive force. Under increasing compressive force (compression phase, upper solid line in Figure 2(a)) the curves become gradually steeper; moreover it has been observed that, under very high forces, the paths become asymptotic to a vertical line, which represents the limit of joint closure.

The overlap represents a mathematically convenient way of measuring relative normal displacement, whose maximum value depends on the height of macro-asperities at contact surfaces. There is also a limiting compressive strength,  $\bar{\Lambda}_n$ , for the contact. If the compressive strength is exceeded, then local failure occurs and numerical contact is lost.

On decompression (expansion phase, lower solid line in Figure 2(a)), the jointed blocks show markedly hysteretic behaviour. The unloading contact force envelope curves for joints are also hyperbolic.<sup>14</sup> Behaviour is governed by equation (23) as for the compression phase, assuming an initial stiffness smaller than that one in compression; thus, the compression and expansion envelope curves can be represented by the following equations (see equation (23)):

$$\begin{aligned} \Lambda_n^C(u_n) &= k_{ni}^C U_n \frac{u_n}{u_n - U_n} \\ \Lambda_n^E(u_n) &= k_{ni}^E U_n \frac{u_n}{u_n - U_n} \\ k_{ni}^E &\leq k_{ni}^C \end{aligned} \quad (25)$$

The quantities  $k_{ni}^C$  and  $k_{ni}^E$  are the initial stiffnesses of the compression and expansion envelope curves, respectively, for  $u_n \geq 0$  separation occurs and hence contact forces drop to zero. The compression and expansion envelope curves are limit curves, whose analytical form is to be determined by imposing to cross the origin with given stiffnesses and to tend asymptotically to the limiting overlap.

For different initial conditions, loading (in compression) and unloading (in expansion) curves relating contact force and relative displacement are used in the present study, Figure 2(a) (dashed lines), as follows:

$$\begin{aligned}\lambda_n^C(u_n) &= \Lambda_n^C(u_n) - [\Lambda_n^C(u_n) - \lambda_n^C(u_n^0)] \exp^{-\gamma_c(u_n - u_n^0)/(u_n - U_n)}, \quad u_n < u_n^0 \\ \lambda_n^E(u_n) &= \Lambda_n^E(u_n) + [\lambda_n^E(u_n^0) - \Lambda_n^E(u_n)] \exp^{-\gamma_e(u_n - u_n^0)/u_n}, \quad u_n > u_n^0 \\ \lambda_n(u_n) &= 0, \quad u_n \geq 0,\end{aligned}\tag{26}$$

where  $u_n$  and  $u_n^0$  are the contact overlaps at the current and previous time step, respectively,  $\gamma_c$  and  $\gamma_e$  are model parameters used for describing the rate at which the contact force within a hysteresis loop approaches the corresponding (compression or expansion) envelope curve. As for envelope curves, separation ( $u_n \geq 0$ ) implies  $\lambda_n = 0$ . Equations (26)<sub>1,2</sub> relate step-by-step current contact forces  $\lambda_n(u_n)$ , respectively, in the compression and expansion phases, to the envelope contact forces  $\Lambda_n(u_n)$ , equations (25), and to the contact forces at the end of the previous step  $\lambda_n(u_n^0)$ . Thus, at each time step the storage of two variables  $u_n$  and  $u_n^0$  is required. The inequality  $\gamma_e \leq \gamma_c$  avoids intersections between current loading and unloading branches.

Figure 2(b) shows the behaviour of numerical contact (solid line) under a sinusoidal overlap program (dashed line) of decreasing amplitude, with the following values of the parameters in equations (25) and (26):  $k_{ni}^C = 1000 \text{ kN/m} = 2k_{ni}^E$ ,  $|U_n| = 0.75 \times 10^{-2} \text{ m}$ ,  $\gamma_c = \gamma_e = 5$ ,  $\bar{\Lambda}_n = \infty$ .

#### 4.2. Contact law in tangential direction

The shear strength at the single contact due to macro-asperities along the interfaces is defined as a multistate variable law.<sup>19,20</sup>

$$\begin{aligned}\lambda_t &= -\mu \lambda_n [1 - \exp^{-(\delta|u_t - u_{tr}|)/b}] \text{sign}(\dot{u}_t) \\ \mu &= \tan(\varphi_1 + \varphi_2) \\ \lambda_t &= 0, \quad \lambda_n \leq 0, \quad \dot{u}_t = 0\end{aligned}\tag{27}$$

The slip at the last reversal point is  $u_{tr}$ ,  $\varphi_1$  is the current value of incremental angle due to macro-asperities,  $\varphi_2$  is the current value of residual angle due to micro-asperities,  $\varphi_1 + \varphi_2$  is the peak value of friction angle,  $\delta$  is a non-dimensional parameter governing the slope of the shear strength curve.

Angle  $\varphi_1$  depends on normal force, normal force rate, cumulative relative displacement  $u_{tc}$  and absolute value of the relative speed  $|\dot{u}_t|$  according to the following law:

$$\varphi_1 = \varphi_0 \exp^{-c_n c_t}\tag{28}$$

with  $\varphi_0$  = initial value of incremental angle  $\varphi_1$ ,

$$\begin{aligned} \lambda_n &> 0, \quad \bar{\lambda}_N > 0, \quad \lambda_n \leq \bar{\lambda}_N, \quad \dot{\lambda}_n > 0 \\ C_n &= \left( \frac{\lambda_n}{\bar{\lambda}_N - \lambda_n} \right)^{h_n}, \quad \dot{\lambda}_n \leq \bar{\lambda}_n \Rightarrow h_n = c_n \\ &\quad \dot{\lambda}_n > \bar{\lambda}_n \Rightarrow h_n = c_n \frac{\dot{\lambda}_n}{\bar{\lambda}_n} \\ u_{tC} &= \int_0^t |\dot{u}_t| d\tau, \quad \bar{u}_t > 0 \\ C_t &= \left( \frac{u_{tC}}{\bar{u}_{tC} - u_{tC}} \right)^{h_t}, \quad |\dot{u}_t| \leq \bar{u}_t \Rightarrow h_t = c_t \\ &\quad |\dot{u}_t| > \bar{u}_t \Rightarrow h_t = c_t \frac{|\dot{u}_t|}{\bar{u}_t} \end{aligned}$$

$\bar{u}_{tC}$  is the yield value of cumulative slip, such that, if exceeded, shear damage stops and only residual friction is exhibited by the joint;  $\bar{\lambda}_n, \bar{u}_t$  are yield values of compression and absolute slip rates, respectively, such that, if exceeded, load-rate effect is exhibited by the contact, simulating the influence of impact velocity on shear response of the joint;  $c$  is a non-dimensional parameter governing the slope of the current value of incremental angle due to macro-asperities;  $c_n$  and  $c_t$  are non-dimensional parameters tuning, the compression and slip rates, respectively.

Moreover, the current value of residual angle  $\varphi_2$  deteriorates according to the following law ('aquaplane' effect):

$$\varphi_2 = \varphi_r \exp^{-|u_t|/\tilde{u}_t}, \quad \tilde{u}_t \geq 0 \quad (29)$$

where  $\varphi_r$  is the initial value of residual angle  $\varphi_2$  and  $\tilde{u}_t$  the suitable reference value of slip rate.

Parameters  $\varphi_0, \varphi_r, \bar{u}_{tC}, \bar{\lambda}_n, \bar{u}_t, \tilde{u}_t$  are to be identified on experimental basis. For more details, concerning the experimental identification of the above-mentioned parameters, the reader may refer to Reference 13.

Figures 3 illustrate the sensitivity of monotonic curve to parameters  $c$  and  $\varphi_0$ : Figure 3(a) demonstrate the ability of the model to represent either rough and smooth joints, while Figure 3(b) allows to account for different joint ductility. Figure 4 shows a typical shear-slip curve (black line) of numerical contact for cyclic loading (grey line) under constant normal force. The tangential contacts have been characterized by the following values:  $\varphi_0 = 10^\circ$ ,  $\varphi_r = 20^\circ$ ,  $\delta = 0.12$ ,  $b = 0.12$  m,  $c = 1$ ,  $c_n = 0$ ,  $c_s = 1$ ,  $\bar{u}_t = \tilde{u}_t = \infty$ .

#### 4.3. Physical explanation

Joint surface is characterized by macro-asperities (first-order asperities) and micro-asperities (second order asperities), as shown in Figure 5.<sup>21</sup>

When joint surfaces overlap, the following types of contact can be detected:

(1) First order–first order; (2) second order–second order; (3) first order–second order. External loads cause slip of contacting surfaces which may be damaged. No damage is exhibited if slip takes place after dilatancy occurs, and this is may be the case in all contact types. Damage can occur only in contacts (1) or (3), that is when slip is due to the failure of first order asperities.

Highest shear strength is exhibited by contact (1) and can be associated with the friction angle  $\varphi_1$ . Lowest shear strength is performed by contact (2) and can be related to the residual angle of

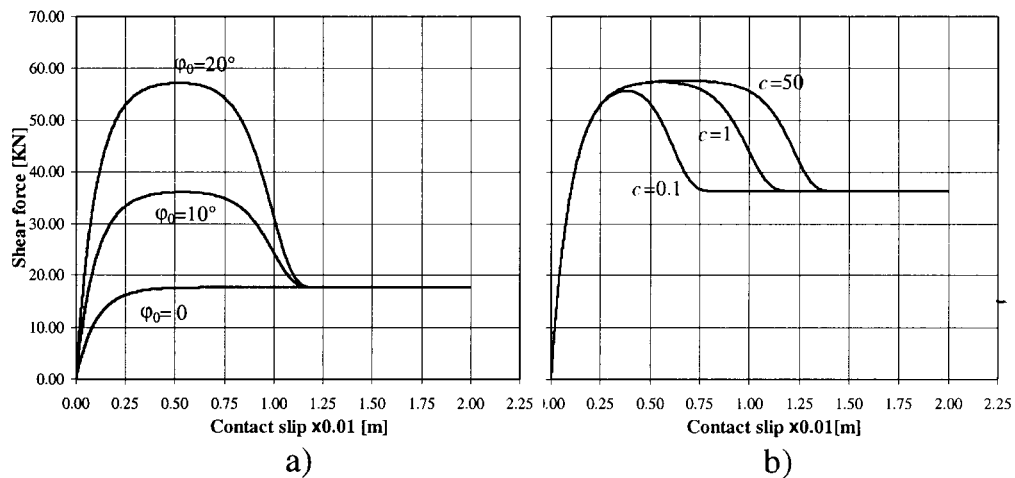


Figure 3. Contact law in tangential direction. (a) Joint roughness; (b) joint ductility

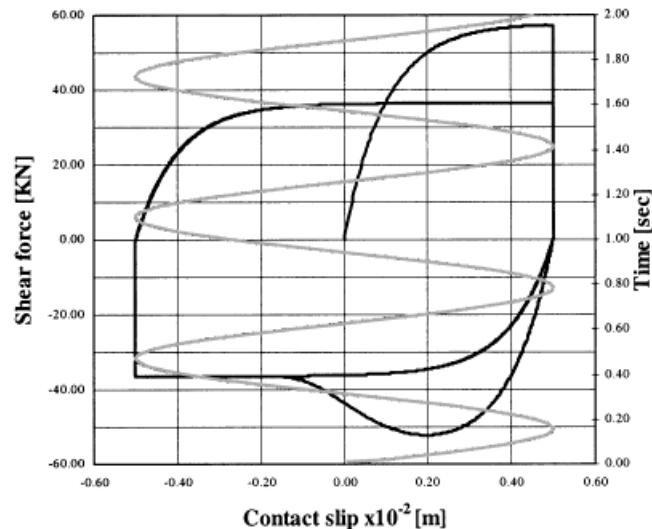


Figure 4. Contact law in tangential direction: behaviour under cyclic slip

friction  $\phi_2$ ; second-order asperities supply residual strength in as much as they represent the ultimate stage in the damage evolution starting from intact first order asperities. Intermediate shear strength is given by contact (3); in this case the manner in which asperities interlock does not differ significantly from that in contact (1): interlocking is limited by the smallest size of contacting asperities. Contact (3) does not exhibit shear strength larger than that of contact (2); thus only contacts (1) and (2) will be considered in the following.

As far as contact (2) is concerned, dilatancy prevails on damage and increases as slip rate increases and as normal force decreases. At contact (1), damage takes place. Then, failure of

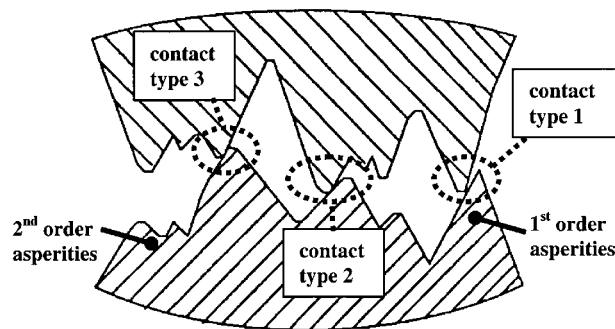


Figure 5. Contact between asperities of two physical contact boundaries<sup>21</sup>

first-order asperities leads to contact (2), where dilatancy prevails and slip rate sensitivity is exhibited. With respect to contact (2) shear strength exhibits a yield value and asymptotically tends to residual shear strength. Damage of yield strength depends on external loading and on cumulated slip. The aquaplane effect occurs only if  $\varphi_1$  is completely erased.

So far, joint surfaces can be modelled by means of a discrete number of contact points. A contact point can represent either a first- or a second-order asperities. Of course, within the range of first- or second-order asperities different sizes can be grouped together and therefore experiments using different strengths can be performed.

## 5. CONCLUSIONS

In this paper a synthetic review concerning the formulation of multibody dynamics with rigid and deformable contacts has been presented. A model of contact forces has been proposed within the framework of the deformable contact formulation. In addition, the theoretical review concerning the formulation of multibody dynamics with rigid contacts has been presented because, in the authors' opinion, it can be used as the mathematical foundation for all the solution algorithms, including those dealing with deformable contact models.

Particular attention has been given to modelling contact-impact phenomena occurring at interaction surfaces between colliding blocks; thus, refined contact force-relative displacement relations have been formulated in order to represent joint behaviour in either normal and tangential directions with respect to the contact surface, accounting for detachment, hysteresis, friction-compression coupling and damage. The proposed model of contact forces is suitable to represent closure and sliding of stone joints.

In Part 2 contact forces between blocks at a discrete number of contact points will be simulated via the proposed model; furthermore, a numerical procedure will be performed in order to analyse the dynamic response of a three-block assembly (trilith).

## ACKNOWLEDGEMENTS

This work was partially funded by the Italian Ministry of University and Scientific Research.

## REFERENCES

1. B. Brogliato, *Nonsmooth Impact Mechanics*, Springer, London, 1996.
2. P. A. Cundall and R. D. Hart, 'Numerical modelling of discontinua', *Engng. Comput.* **9**(2), 101–113 (1992).
3. T. Levi Civita and U. Amaldi, *Lezioni di Meccanica Razionale*, Zanichelli 1927 (in Italian).
4. A. Signorini, *Lezioni di Fisica Matematica*, E. V. Veschi ed., Rome, 1951 (in Italian).
5. J. Pérès, *Mécanique Générale*, Masson et Cie, Paris, 1953 (in French).
6. P. Lötstedt, 'Coulomb Friction in two-dimensional rigid body systems', *ZAMM* **61**, 605–615 (1981).
7. P. Lötstedt, 'Mechanical systems of rigid bodies subject to unilateral constraints', *SIAM. Appl. Math.* **42**(2), 281–296 (1982).
8. J. J. Moreau, 'Unilateral contact and dry friction in finite friction dynamics', in J. J. Moreau and P. D. Panagiotopoulos (eds.), *Non Smooth Mechanics and Applications*, CISM Courses and Lectures, Vol. 302, Springer, Berlin, 1988, pp. 1–82.
9. M. Jean and J. J. Moreau, 'Unilaterality and dry friction in the dynamics of rigid body collections', *Proc. of Contact Mechanics Int. Symp.*, Presses Polytechnique et Universitaires Romandes, Lausanne, 1992, pp. 31–48.
10. P. D. Panagiotopoulos, *Hemivariational Inequalities. Applications in Mechanics and Engineering*, Springer, New York, 1993.
11. F. Pfeiffer and C. Glocker, *Multibody Dynamics with Unilateral Constraints*, Wiley, New York, 1996.
12. A. Sinopoli, 'Unilaterality and dry friction: a geometric formulation for two-dimensional rigid body dynamics', *Nonlinear Dyn.* **12**, 343–366 (1997).
13. U. Andreaus and N. Nisticò, 'An analytical-numerical model for contact-impact problems. Theory and implementation in a 2-Dimensional distinct element algorithm', *Comput. Model. Simulation Engng.* **3**(2), 98–110 (1998).
14. S. C. Bandis, A. C. Lumsden and N. R. Barton, 'Fundamentals of rock joint deformation', *Int. J. Rock Mech. Min. Sci. Geomech. Abstr.* **20**(6), 249–268 (1983).
15. N. R. Barton, S. C. Bandis and K. Bakhtar, 'Strength, deformation and conductivity coupling of rock joints', *Int. J. Rock Mech. Min. Sci. Geomech. Abstr.* **22**(3), 121–140 (1985).
16. E. S. Hwang and A. S. Nowak, 'Simulation of dynamic load for bridges', *J. Struct. Engng. ASCE* **117**(5), 1413–1434 (1991).
17. R. L. Kondner, 'Hyperbolic stress-strain response: cohesive soils', *J. Soil Mech. Fdns. Div. ASCE* **89**(1), 115–143 (1963).
18. J. M. Duncan and C. Y. Chang, 'Non-linear analysis of stress and strain in soils', *J. Soil Mech. Fdns. Div. ASCE* **96**(5), 1629–1653 (1970).
19. N. R. Barton and V. Choubey, 'The shear strength of rock joints in theory and practice', *Rock Mech.* **10**, 1–54 (1977).
20. J. R. Rice and A. L. Ruina, 'Stability of steady frictional slipping', *J. Appl. Mech.* **50**(2), 343–349 (1983).
21. Z. H. Zhong, *Finite Element Procedures for Contact-Impact Problems*, Oxford University Press, Oxford, 1993.